Reprinted from Journal of the Optical Society of America A

Numerical study of the symmetrical strip-grating-loaded slab

R. Petit and G. Tayeb

Laboratoire d'Optique Electromagnétique, 843, Faculté des Sciences et Techniques, Centre de Saint-Jérôme, 13397 Marseille Cedex 13, France

Received March 7, 1989; accepted October 3, 1989

As a result of symmetry considerations, a simple computer code is proposed that permits inexpensive study of some noteworthy properties of the symmetrical strip-grating-loaded slab.

1. COMMENTS ON A PREVIOUSLY PROPOSED METHOD

First, we would like to examine briefly a paper by Lakhtakia *et al.*[1] A critical examination of Ref. 1 has already been published (the reader who did not follow the controversy can go directly to Section 2).

As pertains to Ref. 1, we call a symmetrical strip-grating-loaded slab the structure depicted in Fig. 1. We designate ϵ_0 and μ_0 as the vacuum permittivity and permeability, respectively. In Fig. 1 regions 1 ($z > 2d$) and 3 ($z < 0$) are both filled with a medium whose constitutive parameters are ϵ_1 and μ_0. In region 2 ($0 < z < 2d$) lies the grating medium (ϵ_2, μ_0) divided into cells (width $2a$) by perfectly conducting walls, which are represented by the vertical, heavy lines. If the structure is illuminated in normal incidence by a monochromatic plane wave (wavelength in vacuum λ_0) and we take into account a time dependence in $\exp(-i\omega t)$, the total field in region 1 is given by

$$\psi_1(x, z) = \sum_{n=0}^{2N} [A_n^- \exp(-i\beta_{1n}z) + A_n^+ \exp(i\beta_{1n}z)] \times \exp[i(n - N)\pi x/a], \quad (1)$$

with

$$\beta_{1n} = \{k_1^2 - [(n - N)\pi/a]^2\}^{1/2}, \qquad A_n^- = \delta_{nN}. \quad (1')$$

Likewise, in region 3 the total field can be represented as

$$\psi_3(x, z) = \sum_{n=0}^{2N} C_n^- \exp(-i\beta_{1n}z)\exp[i(n - N)\pi x/a]. \quad (2)$$

Finally, and by assuming TE polarization for simplicity, the field is given in region 2 by the modal representation

$$\psi_2(x, z) = \sum_{n=0}^{2N} [B_n^- \exp(-i\beta_{2n}z) + B_n^+ \exp(i\beta_{2n}z)] \times \sin\left[(n + 1)\pi \frac{x + a}{2a}\right], \quad (3)$$

$$\beta_{2n} = \left\{k_2^2 - \left[\frac{(n + 1)\pi}{2a}\right]^2\right\}^{1/2}. \quad (3')$$

To obtain the unknowns A_n^+, B_n^+, B_n^-, and C_n^-, we must write the continuities of the field and of the z derivative at $z = 0$ and $z = 2d$. To this end, and as was done in Ref. 1, we can express the equality of two functions by equalizing their components on the basis formed by functions $\sin[(n + 1)\pi(x + a)/2a]$. It is convenient to introduce column matrices A^-, A^+, B^+, B^-, and C^-, whose components are, respectively, A_n^-, A_n^+, B_n^+, B_n^-, and C_n^-. The matching at $z = 0$ leads to

$$a(B^- + B^+) = JC^-, \quad (4)$$

$$a(-B^- + B^+) = -M_2^{-1}JM_1C^-. \quad (4')$$

The matching at $z = 2d$ leads to

$$a(D_2^-B^- + D_2^+B^+) = JD_1^-A^- + JD_1^+A^+, \quad (5)$$

$$a(-M_2D_2^-B^- + M_2D_2^+B^+) = -JM_1D_1^-A^- + JM_1D_1^+A^+, \quad (5')$$

where D_1^+, D_1^-, D_2^+, D_2^-, M_1, and M_2 are diagonal matrices with elements $\exp(i\beta_{1n}2d)\delta_{m,n}$, $\exp(-i\beta_{1n}2d)\delta_{m,n}$, $\exp(i\beta_{2n}2d)\delta_{m,n}$, $\exp(-i\beta_{2n}2d)\delta_{m,n}$, $\beta_{1n}\delta_{m,n}$, and $\beta_{2n}\delta_{m,n}$, respectively. The expression for $J_{m,n}$ is given in Appendix A.

As was already mentioned in Ref. 2, we agree with Lakhtakia *et al.* for the matching at $z = 0$ only [Eqs. (4) and (4')]. Our Eqs. (5) and (5') are different from their Eq. (9) found in Ref. 1. Finding A^+ and C^- is a simple but tedious problem. Starting with Eqs. (4), (4'), (5), and (5') and eliminating B^+ and B^- yields

$$C^- = 4MD_1^-A^-, \quad (6)$$

$$A^+ = D_1^-PM^{-1}D_1^-A^-, \quad (7)$$

where M and P are deduced from the preceding matrices as follows:

$$M = X_1 - X_2 - X_3 + X_4, \qquad P = X_1 - X_2 + X_3 - X_4,$$
$$X_1 = J^{-1}SJ, \qquad X_2 = J^{-1}DM_2^{-1}JM_1,$$

0740-3232/90/030373-06$02.00

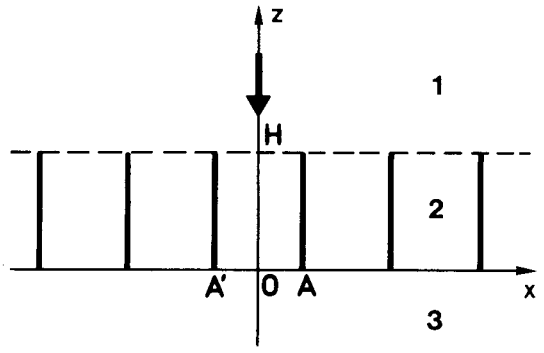

Fig. 1. $\overline{OH} = 2d$, $\overline{A'A} = 2(\overline{A'O}) = 2a$. Regions 1 and 3 are filled with the same medium.

$$X_3 = M_1^{-1}J^{-1}M_2DJ, \qquad X_4 = M_1^{-1}J^{-1}SJM_1,$$
$$S = D_2^{+} + D_2^{-}, \qquad D = D_2^{+} - D_2^{-}.$$

Most readers will probably not try to verify all these equations! Although there are many opportunities to make a mistake, we hope they are exact because the numerical results we got from Eqs. (6) and (7) are identical to those obtained from the much more simple and reliable algorithm described in Section 2. We must emphasize that because MD_1^{-} is not a diagonal matrix, the transmitted field is not purely specular as claimed in Ref. 1. Moreover, from Eq. (7), the reflected field A^{+} does not vanish in the general case.

2. THE METHOD THAT WE SUGGEST

A. Generalities

In Section 1 we endeavored to use the same notations as in Ref. 1. Now, we will use notations with which we are more familiar. We therefore choose a new coordinate system (Fig. 2). The thickness will be denoted $2h$, and d will be the pitch of the grating. Moreover, we will deal with an arbitrary incidence angle θ ($0 \leqslant \theta < \pi/2$). What we call the total field u is the z component of **E** or **H**, depending on whether the polarization is TE or TM. When the incident field is written in the form $u^i(x, y) = \exp[-i\beta_0(y - h) + i\alpha_0 x]$, $u(x, y)$ in region 1 can be described by

$$u(x, y) = u^i(x, y) + \sum_{n=-\infty}^{+\infty} R_n \psi_n{}^r(x, y) \tag{8}$$

and $u(x, y)$ in region 3 by

$$u(x, y) = \sum_{n=-\infty}^{+\infty} T_n \psi_n{}^t(x, y), \tag{9}$$

where

$$\psi_n{}^r = \exp[i\beta_n(y - h) + i\alpha_n x],$$
$$\psi_n{}^t = \exp[-i\beta_n(y + h) + i\alpha_n x],$$
$$\alpha_n = \omega\sqrt{\epsilon_1\mu_0}\sin\theta + n(2\pi/d),$$
$$\beta_n{}^2 = \omega^2\epsilon_1\mu_0 - \alpha_n{}^2, \qquad \beta_n \text{ or } \beta_n/i > 0. \tag{10}$$

For now it is not necessary to specify the form of $u(x, y)$ in region 2.

It is convenient to introduce two problems, problems P_s and P_a, for which the total field is, respectively, symmetric and antisymmetric. These problems and their associated fields are described in Fig. 3. Notice that $(\partial u/\partial y)(x, 0) = 0$ in problem P_s, whereas $u(x, 0) = 0$ in problem P_a. Therefore, from the superposition principle

$$R_n = (A_n + B_n)/2, \qquad T_n = (A_n - B_n)/2. \tag{11}$$

B. TE Polarization

In region 2 and for $0 \leqslant x \leqslant d$, the total field $u(x, y)$, which vanishes for $x = 0$ and $x = d$, can be expanded on the basis of functions $f_n(x) = \sin(n\pi x/d)$, where n varies from 1 to infinity:

$$u(x, y) = \sum_{n=1}^{\infty} u_n(y) f_n(x). \tag{12}$$

From the Helmholtz equation, it turns out that

$$u_n(y) = a_n \sin(\sigma_n y) + b_n \cos(\sigma_n y), \tag{13}$$

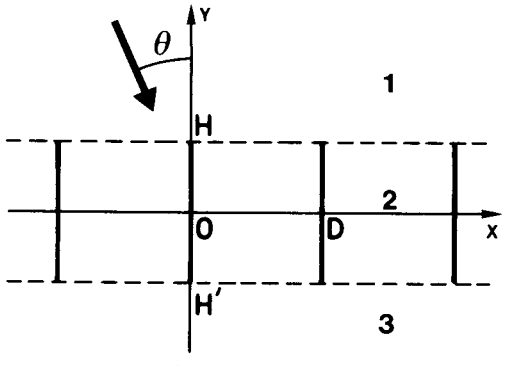

Fig. 2. $\overline{OH} = \overline{H'O} = h$, $\overline{OD} = d$.

	region 1	region 3
1, (P)	$u^i(x,y) + \sum R_n \psi_n^r(x,y)$	$\sum T_n \psi_n^t(x,y)$
1, 1, (P_s)	$u^i(x,y) + \sum A_n \psi_n^r(x,y)$	$u^i(x,-y) + \sum A_n \psi_n^t(x,y)$
1, -1, (P_a)	$u^i(x,y) + \sum B_n \psi_n^r(x,y)$	$-u^i(x,-y) - \sum B_n \psi_n^t(x,y)$

Fig. 3. The field description in regions 1 and 3 for the initial problem P and the problems P_s and P_a.

where

$$\sigma_n{}^2 = \omega^2\epsilon_2\mu_0 - (n\pi/d)^2. \tag{13'}$$

In problem P_s and because $u_n'(0)$ vanishes, the a_n coefficients are null. We perform the matching at $y = h$ (continuity of u and $\partial u/\partial y$ by projection on the basis of f_n), thus obtaining

$$b_n \cos(\sigma_n h) = \sum_m K_{nm}(\delta_{0m} + A_m), \tag{14}$$

$$i\sigma_n b_n \sin(\sigma_n h) = \sum_m K_{nm}\beta_m(-\delta_{0m} + A_m), \tag{14'}$$

with (see Appendix B for more details)

$$K_{nm} = \frac{2}{d}\int_0^d \exp(i\alpha_m x)\sin(n\pi x/d)\mathrm{d}x. \tag{15}$$

When the field symmetry is taken into account, the matching at $y = -h$ is automatically achieved. After truncation and elimination of the b_n between Eq. (14) and Eq. (14'), we obtain a linear system of $2N + 1$ equations for the $2N + 1$ unknowns $A_m(-N \leqslant m \leqslant +N)$:

$$\sum_{m=-N}^{+N} M_{nm}A_m = S_n, \qquad n = 1, 2N + 1, \tag{16}$$

$$M_{nm} = [\beta_m - i\sigma_n \tan(\sigma_n h)]K_{nm}, \tag{17}$$

$$S_n = [\beta_0 + i\sigma_n \tan(\sigma_n h)]K_{n0}. \tag{18}$$

In problem P_a and because $u_n(0)$ vanishes, it is the b_n coefficients that are null. It is easy to verify that the matching at $y = h$ leads to the same linear system [Eqs. (16)–(18)] except that we have to replace A_m by B_m and $\tan(\sigma_n h)$ by $-\cot(\sigma_n h)$.

Looking again at problem P, we can see that the Rayleigh coefficients R_n and T_n are given by Eqs. (11). Let us recall[3] that because we use the same basis to express the continuity of u and of $\partial u/\partial y$, the energy-balance criterion can be used to check the quality of the approximate solution obtained after truncature.

C. TM Polarization

In this case, $\partial u/\partial x$ must vanish for $x = 0$ and $x = d$. Consequently, in region 2 and for $0 \leqslant x \leqslant d$, $u(x, y)$ is now expanded on the basis of functions $g_n(x) = \cos(n\pi x/d)$, where n varies from 0 to infinity:

$$u(x, y) = \sum_{n=0}^{\infty} u_n(y)g_n(x). \tag{19}$$

From the Helmholtz equation, we see that the functions $u_n(y)$ are still given by Eqs. (13) and (13').

In problem P_s the a_n coefficients still vanish. We now perform the matching at $y = h$ [continuity of u and $(\partial u/\partial y)/\epsilon(y)$] by projection on the basis of g_n. We obtain

$$b_n \cos(\sigma_n h) = \sum_m \tilde{K}_{nm}(\delta_{0m} + A_m), \tag{20}$$

$$b_n \frac{\sigma_n}{\epsilon_2}\sin(\sigma_n h) = \sum_m i\frac{\beta_m}{\epsilon_1}\tilde{K}_{nm}(\delta_{0m} - A_m). \tag{21}$$

The expression for $\tilde{K}_{nm}$ is given in Appendix B. As in the TE case, we obtain a linear system:

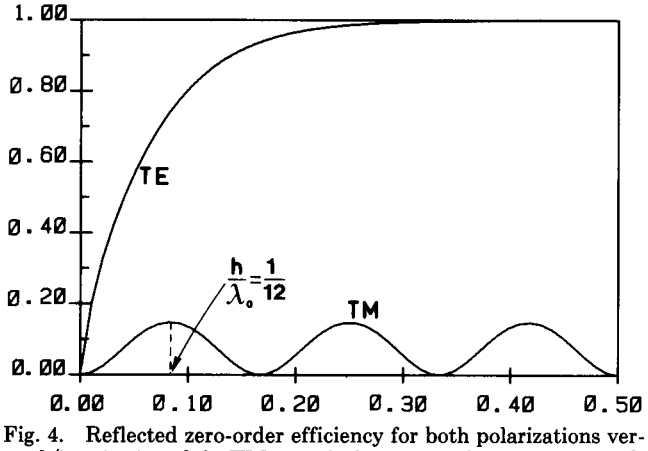

Fig. 4. Reflected zero-order efficiency for both polarizations versus h/λ_0. $\theta = 0$, and the TM curve is the same as the one corresponding to the bare slab, as noted in Ref. 2. $d/\lambda_0 = 0.3$ (no influence in TM), $\epsilon_1 = \epsilon_0$, $\epsilon_2/\epsilon_0 = 2.25$.

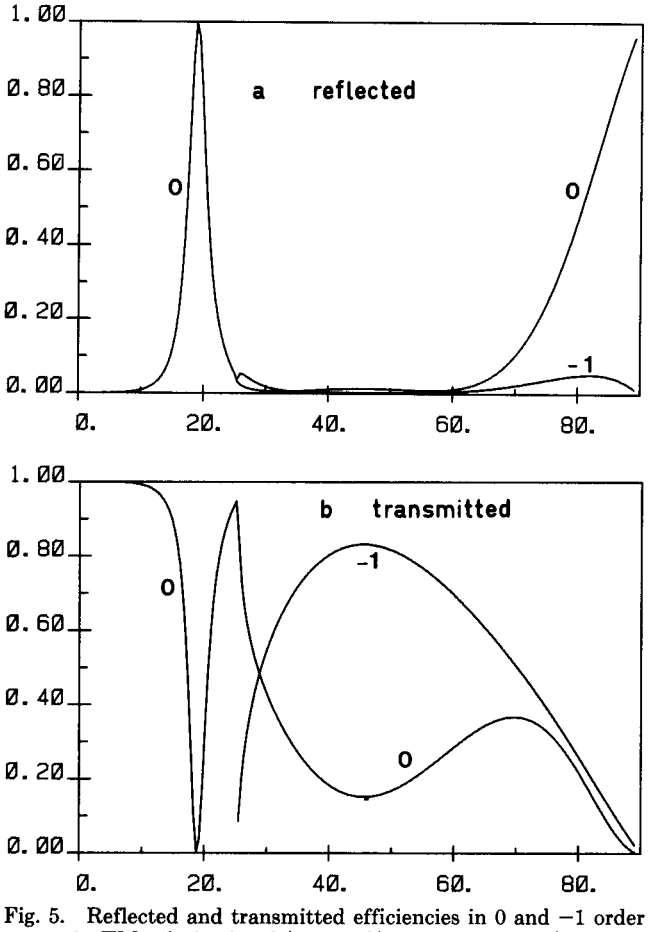

Fig. 5. Reflected and transmitted efficiencies in 0 and −1 order versus θ: TM polarization, $h/\lambda_0 = 1$, $d/\lambda_0 = 0.7$, $\epsilon_1 = \epsilon_0$, $\epsilon_2/\epsilon_0 = 2.25$.

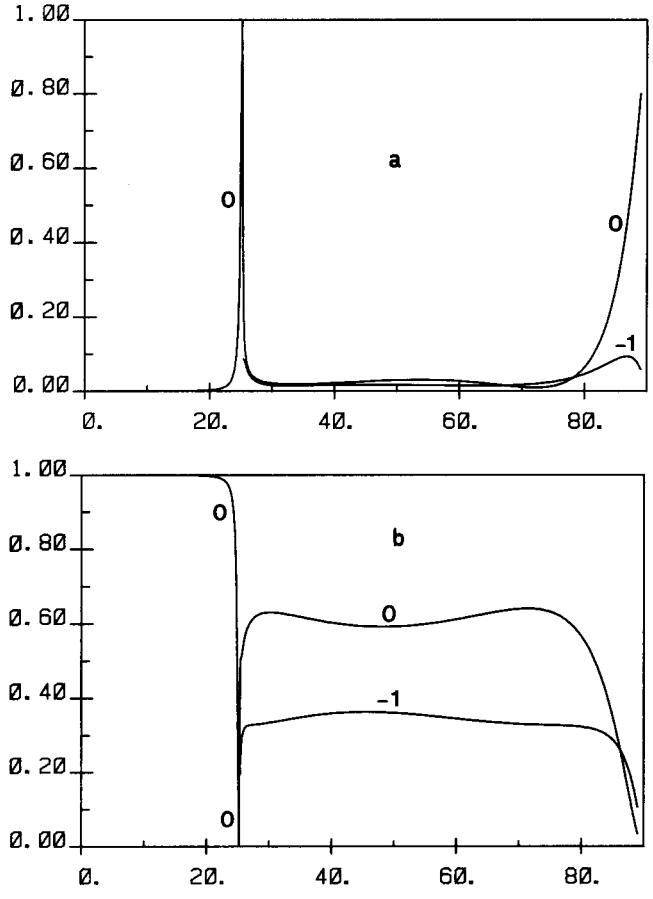

Fig. 6. Same as Fig. 5 for $h/\lambda_0 = 5$.

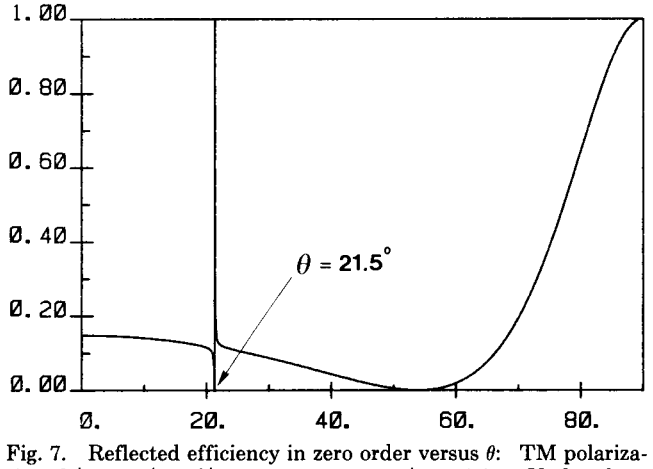

Fig. 7. Reflected efficiency in zero order versus θ: TM polarization, $h/\lambda_0 = 1/12$, $d/\lambda_0 = 0.7$, $\epsilon_1 = \epsilon_0$, $\epsilon_2/\epsilon_0 = 2.25$. Under these conditions, the efficiencies in the -1 reflected and transmitted orders that appear for $\theta = 25.4°$ are always less than 0.001. The h/λ_0 value (1/12) gives a maximum of reflection in normal incidence (see Fig. 4).

$$\sum_{m=-N}^{+N} \tilde{M}_{nm} A_m = \tilde{S}_n, \qquad n = 0, 2N, \tag{22}$$

$$\tilde{M}_{nm} = \left[\frac{\beta_m}{\epsilon_1} - i\frac{\sigma_n}{\epsilon_2}\tan(\sigma_n h)\right]\tilde{K}_{nm}, \tag{23}$$

$$\tilde{S}_n = \left[\frac{\beta_0}{\epsilon_1} + i\frac{\sigma_n}{\epsilon_2}\tan(\sigma_n h)\right]\tilde{K}_{n0}. \tag{24}$$

In problem P_a, the B_m values are again obtained by a linear system that is the same as that for Eqs. (22)–(24), except that we must replace A_m by B_m and $\tan(\sigma_n h)$ by $-\cot(\sigma_n h)$.

The Rayleigh coefficients of problem P are still given by Eqs. (11).

D. Numerical Implementation and Results

This method, which benefits from symmetry considerations, is easy to implement on a computer and even on a microcomputer because of the short computation time. For a given polarization, this method reduces to the solving of two linear systems whose coefficients are given in closed form. Indeed, the computer code that we have written seems efficient and reliable.

This program was first used to check the validity of Eqs. (6) and (7). It provides us with data that do not confirm the strange behavior pointed out in Ref. 1. They do, however, show agreement with the properties expected by microwave researchers. For example, when $2d$ is less than the wavelength in the grating medium, the strip-grating-loaded slab exhibits strong polarization properties because of the lack of transmission observed in TE polarization for a sufficient thickness $2h$ (Fig. 4). Let us now look at Fig. 5, which corresponds to TM polarization. On reflection, the zero-order efficiency, which is low for a large range of θ, presents, in the vicinity of 19° (see Appendix C), a peak of 100%. This same phenomenon, which is more strongly marked, can be observed in Figs. 6 and 7. In other words, for a fixed wavelength such a grating acts as a perfect mirror for a particular incidence and as a transmission grating for the other incidences. Conversely, for a given incidence the reflection peak occurs for a particular value of the wavelength (Fig. 8), as was noted previously by several authors.[4–6]

We hope that the real simplicity of the method suggested in this paper will be attractive for engineers and more generally for any person not familiar with the subtleties of Wiener–Hopf-type methods.[5] Undoubtedly, an extensive numerical study would lead to interesting and numerous appli-

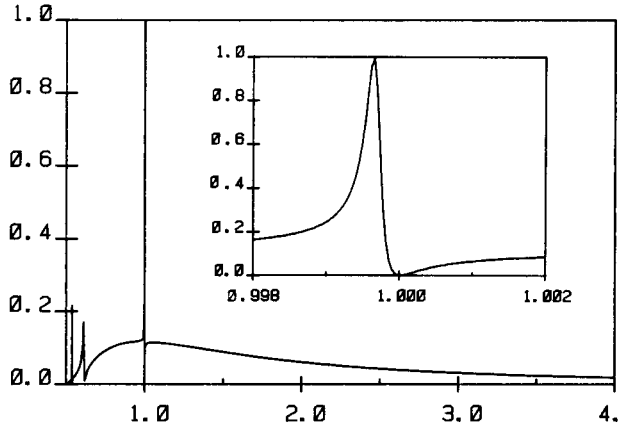

Fig. 8. Reflected efficiency in zero order versus λ_0: TM polarization, $h = 1/12$, $d = 0.7$, $\epsilon_1 = \epsilon_0$, $\epsilon_2/\epsilon_0 = 2.25$, $\theta = 21.5°$. Only the zero order exists if $\lambda_0 > 0.954$. The enlargement shows the resonance peak with more details.

cations for any range of wavelengths for which the hypothesis of an infinite conductivity is reasonable (i.e., far infrared, microwaves).

To conclude, we offer our opinion on the controversy between Kobayashi[5] and Montgomery[6] on the one hand and Kent and Lee[4] on the other hand. All these authors studied the same structure ($d/\lambda_0 = 0.75$, $h/\lambda_0 = 0.5$, $\epsilon_1 = \epsilon_2 = \epsilon_0$) and plotted $|R_0|$ versus θ. The total reflection angle θ_0 is approximately 16° according to Refs. 5 and 6 and 13° according to Ref. 4. We found this value to be approximately 15.5°, but we confess that obtaining a reliable value for θ_0 requires a great value of the truncation number N (our estimate is, respectively, 14.8°, 15.2°, 15.4°, and 15.5° for $N = 5$, 10, 15, and 20). Fortunately, apart from this sharp phenomenon, the results are not so sensitive to the value of N, and we found that $N = 5$ is sufficient for most calculations.

APPENDIX A

The elements of matrix J are

$$J_{m,n} = \int_{-a}^{a} \exp[i(n-N)\pi x/a]\sin\left[(m+1)\pi\frac{x+a}{2a}\right]dx.$$

Setting

$$J(\alpha) = \frac{1}{2ia}\int_{-a}^{+a}\exp(i\alpha\pi x/a)dx = \begin{cases} -i & \alpha = 0 \\ -i\dfrac{\sin(\alpha\pi)}{\alpha\pi} & \alpha \neq 0 \end{cases},$$

we find that

$$J_{m,n} = a\{\exp[i(m+1)\pi/2]\}J\left(n-N+\frac{m+1}{2}\right) - a\{\exp[-i(m+1)\pi/2]\}J\left(n-N-\frac{m+1}{2}\right).$$

APPENDIX B

We define K_{nm} and $\tilde{K}_{nm}$ as

$$K_{nm} = \frac{2}{d}\int_0^d \exp(i\alpha_m x)\sin(n\pi x/d)dx,$$

$$\tilde{K}_{0m} = \frac{1}{d}\int_0^d \exp(i\alpha_m x)dx,$$

$$\tilde{K}_{nm} = \frac{2}{d}\int_0^d \exp(i\alpha_m x)\cos(n\pi x/d)dx, \qquad n \neq 0.$$

Setting

$$K(t) = \frac{1}{d}\int_0^d \exp(itx)dx = \begin{cases} 1 & t = 0 \\ \dfrac{\exp(idt)-1}{idt} & t \neq 0 \end{cases},$$

we obtain

$$K_{nm} = -i[K(\alpha_m + n\pi/d) - K(\alpha_m - n\pi/d)],$$
$$\tilde{K}_{0m} = K(\alpha_m),$$
$$\tilde{K}_{nm} = K(\alpha_m + n\pi/d) + K(\alpha_m - n\pi/d), \qquad n \neq 0.$$

APPENDIX C

When we examine the zero-order reflected efficiency curve (Figs. 5–8), we might wonder whether the efficiency actually reaches 100%. The answer can be given from considerations similar to those developed in Ref. 7.

Consider the grating depicted in Fig. 2 and illuminated in regions 1 and 3 by two plane waves (complex amplitudes a_1 and a_2) under the same incidence θ (Fig. 9). Provided that $\lambda_1/d > 1 + \sin\theta$, the grating yields two diffracted waves only (amplitudes b_1 and b_2). Let S be the scattering matrix

$$\begin{pmatrix} b_1 \\ b_2 \end{pmatrix} = S\begin{pmatrix} a_1 \\ a_2 \end{pmatrix}.$$

When R_0 and T_0 are defined as in Subsection 2.A, the elements S_{ij} of S are

$$S_{11} = S_{22} = R_0, \qquad S_{12} = S_{21} = T_0.$$

Because S is a unitary matrix, its inverse is equal to its Hermitian adjoint, which indicates that

$$R_0\overline{R_0} + T_0\overline{T_0} = 1, \qquad \mathrm{Re}(R_0\overline{T_0}) = 0.$$

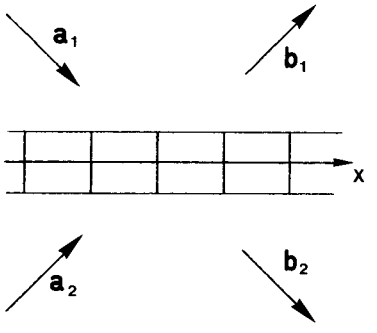

Fig. 9. Grating arrangement described in Appendix C.

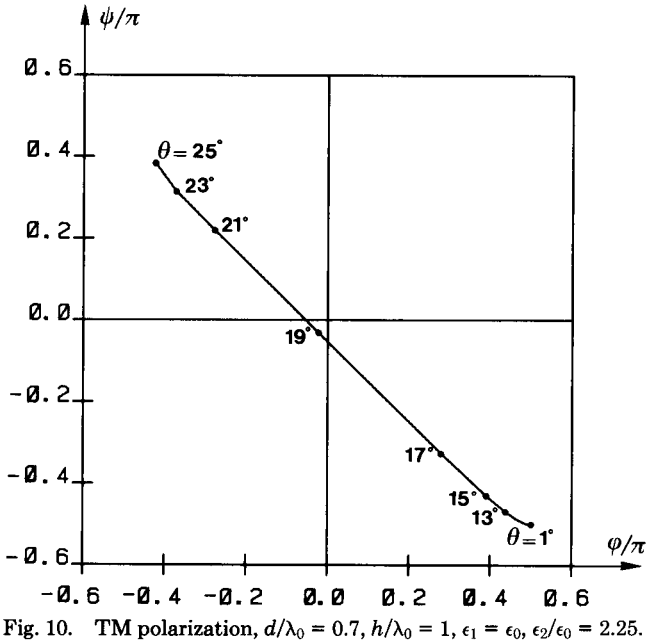

Fig. 10. TM polarization, $d/\lambda_0 = 0.7$, $h/\lambda_0 = 1$, $\epsilon_1 = \epsilon_0$, $\epsilon_2/\epsilon_0 = 2.25$. When θ varies from 1° to 25°, the trajectory $\mathcal{C}$ of point A cuts the $\varphi = 0$ axis.

Consequently, it is convenient to introduce two real parameters φ ($-\pi/2 \leqslant \varphi \leqslant \pi/2$) and ψ ($-\pi < \psi \leqslant \pi$), unambiguously linked with R_0 and T_0 by

$$R_0 = \cos\varphi e^{i\psi}, \qquad T_0 = i \sin\varphi e^{i\psi}.$$

To each incidence θ (Figs. 5–7) or to each value of λ_0 (Fig. 8), we can associate a point $A(\varphi, \psi)$. To claim that the reflected efficiency reaches 100% means that point A crosses the $\varphi = 0$ axis in the φ, ψ plane. Insofar as the trajectory $\mathcal{C}$ (Fig. 10) is assumed to be a continuous curve, we have only to compute a few points to be convinced.

ACKNOWLEDGMENTS

We thank M. Cadilhac, who drew our attention to a paper he wrote some years ago in collaboration with D. Maystre[7] and who helped us with the wording of Appendix C. Appendix C is nothing other than an adaptation of the ideas developed in Ref. 7.

REFERENCES

1. A. Lakhtakia, V. V. Varadan, and V. K. Varadan, "Nontrivial grating that possesses only specular characteristics: normal incidence," J. Opt. Soc. Am. A **3,** 1788–1793 (1986).
2. R. Petit and M. Cadilhac, "On the properties of the strip-grating-loaded slab," J. Opt. Soc. Am. A **6,** 1955–1957 (1989).
3. J. Y. Suratteau, M. Cadilhac, and R. Petit, "Sur la détermination numérique des efficacités de certains réseaux diélectriques profonds," J. Opt. **14,** 273–288 (1983).
4. W. H. Kent and S. W. Lee, "Diffraction by an infinite array of parallel strips," J. Math. Phys. **13,** 1926–1930 (1972).
5. K. Kobayashi, "Diffraction of a plane electromagnetic wave by a parallel plate grating with dielectric loading: the case of transverse magnetic incidence," Can. J. Phys. **63,** 453–465 (1985).
6. J. P. Montgomery, "Scattering by an infinite array of multiple parallel strips," IEEE Trans. Antennas Propag. **27,** 798 (1979).
7. D. Maystre and M. Cadilhac, "A phenomenological theory for gratings: perfect blazing for polarized light in nonzero deviation mounting," Radio Sci. **16,** 1003–1008 (1981).